AFRL-RQ-WP-TP-2013-0242

HIFiRE-5 FLIGHT TEST PRELIMINARY RESULTS (POSTPRINT)

Roger Kimmel, David Adamczak, and Thomas J. Juliano

Hypersonic Sciences Branch
High Speed Systems Division

NOVEMBER 2013

AIR FORCE RESEARCH LABORATORY
AEROSPACE SYSTEMS DIRECTORATE
WRIGHT-PATTERSON AIR FORCE BASE, OH 45433-7542
AIR FORCE MATERIEL COMMAND
UNITED STATES AIR FORCE

NOTICE AND SIGNATURE PAGE

AFRL-RQ-WP-TP-2013-0242 HAS BEEN REVIEWED AND IS APPROVED FOR PUBLICATION IN ACCORDANCE WITH ASSIGNED DISTRIBUTION STATEMENT.

*//Signature//	//Signature//
ROGER L. KIMMEL	MARK AMENDT, Chief
Project Manager	Hypersonic Sciences Branch
Hypersonic Sciences Branch	High Speed Systems Division
High Speed Systems Division	Aerospace Systems Directorate

*Disseminated copies will show "//Signature//" stamped or typed above the signature blocks.

REPORT DOCUMENTATION PAGE

Form Approved
OMB No. 0704-0188

1. REPORT DATE *(DD-MM-YY)*	2. REPORT TYPE	3. DATES COVERED *(From - To)*
November 2013	Conference Paper Postprint	12 April 2012 – 01 January 2013

4. TITLE AND SUBTITLE
HIFiRE-5 FLIGHT TEST PRELIMINARY RESULTS (POSTPRINT)

5a. CONTRACT NUMBER
In-house

5b. GRANT NUMBER

5c. PROGRAM ELEMENT NUMBER
61102F

6. AUTHOR(S)
Roger Kimmel, David Adamczak, and Thomas J. Juliano

5d. PROJECT NUMBER
2307

5e. TASK NUMBER

5f. WORK UNIT NUMBER
Q042

7. PERFORMING ORGANIZATION NAME(S) AND ADDRESS(ES)
Hypersonic Sciences Branch (AFRL/RQHF)
High Speed Systems Division, Air Force Research Laboratory
Aerospace Systems Directorate
Wright-Patterson Air Force Base, OH 45433-7542
Air Force Materiel Command, United States Air Force

8. PERFORMING ORGANIZATION REPORT NUMBER
AFRL-RQ-WP-TP-2013-0242

9. SPONSORING/MONITORING AGENCY NAME(S) AND ADDRESS(ES)
Air Force Research Laboratory
Aerospace Systems Directorate
Wright-Patterson Air Force Base, OH 45433-7542
Air Force Materiel Command
United States Air Force

10. SPONSORING/MONITORING AGENCY ACRONYM(S)
AFRL/RQHF

11. SPONSORING/MONITORING AGENCY REPORT NUMBER(S)
AFRL-RQ-WP-TP-2013-0242

12. DISTRIBUTION/AVAILABILITY STATEMENT
Approved for public release; distribution unlimited.

13. SUPPLEMENTARY NOTES
PA Case Number: 88ABW-2012-6293; Clearance Date: 29 Nov 2012. This paper contains color. The conference paper was presented at the 51st AIAA Aerospace Sciences Meeting including the New Horizons Forum and Aerospace Exposition, held in Grapevine, Texas from January 7 through 10, 2013, and was published in the Proceedings of the 51st AIAA Aerospace Sciences Meeting including the New Horizons Forum and Aerospace Exposition.

14. ABSTRACT
The Hypersonic International Flight Research Experimentation (HIFiRE) program is a hypersonic flight test program executed by the Air Force Research Laboratory (AFRL) and Australian Defence Science and Technology Organisation (DSTO). HIFiRE flight five flew in April 2012. Principle goals of this flight were to measure hypersonic boundary-layer transition on a three-dimensional body. The second stage booster on this flight failed to ignite, so the experiment reached a maximum Mach number of only 3. Nevertheless, supersonic pressure and temperature data were obtained under laminar and turbulent flow, and flight systems were validated. HIFiRE-5 was the first HIFiRE flight to use both the Inertial Sciences Digital Miniature Attitude Reference System (DMARS-R) IMU and Ashtech DG14 Global Positioning System receiver. Results show that a tripped transition occurred on the test article leading edge, but the rest of the configuration showed no gross effects of tripping, with a transition pattern consistent with prior wind tunnel measurements and CFD.

15. SUBJECT TERMS
Boundary layer transition, hypersonic, flight test

16. SECURITY CLASSIFICATION OF:			17. LIMITATION OF ABSTRACT:	18. NUMBER OF PAGES	19a. NAME OF RESPONSIBLE PERSON (Monitor)
a. REPORT	b. ABSTRACT	c. THIS PAGE			Roger L. Kimmel
Unclassified	Unclassified	Unclassified	SAR	22	19b. TELEPHONE NUMBER *(Include Area Code)* N/A

51st AIAA Aerospace Sciences Meeting including the New Horizons Forum and Aerospace Exposition
07 - 10 January 2013, Grapevine (Dallas/Ft. Worth Region), Texas

AIAA 2013-0377

HIFiRE-5 Flight Test Preliminary Results

Roger L. Kimmel* David Adamczak†, Thomas J. Juliano‡

Air Force Research Laboratory, 2130 8th St., WPAFB, OH 45433, USA

DSTO AVD Brisbane Team
Air Vehicles Division, Defence Science and Technology Organisation, PO Box 883 Kenmore, 4069 Australia

The Hypersonic International Flight Research Experimentation (HIFiRE) program is a hypersonic flight test program executed by the Air Force Research Laboratory (AFRL) and Australian Defence Science and Technology Organisation (DSTO). HIFiRE flight five flew in April 2012. Principle goals of this flight were to measure hypersonic boundary-layer transition on a three-dimensional body. The second stage booster on this flight failed to ignite, so the experiment reached a maximum Mach number of only 3. Nevertheless, supersonic pressure and temperature data were obtained under laminar and turbulent flow, and flight systems were validated. HIFiRE-5 was the first HIFiRE flight to use both the Inertial Sciences Digital Miniature Attitude Reference System (DMARS-R) IMU and Ashtech DG14 Global Positioning System receiver. Results show that a tripped transition occurred on the test article leading edge, but the rest of the configuration showed no gross effects of tripping, with a transition pattern consistent with prior wind tunnel measurements and CFD.

Nomenclature

Symbols

p = freestream pressure, kPa
$\dot{q}$ = heat transfer rate, kW/m^2
Re = freestream unit Reynolds number per meter, $\rho_\infty U_\infty/\mu_\infty$
t = time after lift-off, seconds
x = distance from stagnation point along vehicle centerline, m (Figure 2)
y = vertical (pitch-plane) coordinate, m (Figure 2)
z = spanwise (yaw-plane) coordinate, m (Figure 2)
α = vehicle angle of attack relative to wind, degrees (Figure 9)
β = vehicle yaw angle relative to wind, degrees (Figure 9)
Δ = differential between points 180-deg opposite on test article
θ = vehicle instantaneous pitch angle relative to earth as measured by IMU, or flight-path elevation angle as measured by GPS or IMU, degrees
ϕ = body-fixed angular coordinate around vehicle circumference, $\phi = 0$ on centerline ray (minor axis), degrees (Figure 2)
ψ = vehicle instantaneous azimuth angle relative to earth as measured by IMU, or flight-path azimuth angle as measured by GPS or IMU, degrees
ρ = density, kg/m^3
μ = viscosity, N s / m^2

---

* Principal Aerospace Engineer, Associate Fellow AIAA.
† Senior Engineer, Member AIAA
‡ Research Associate, Member, AIAA
Approved for public release, distribution is unlimited, 29 Nov 2012, 88ABW-2012-6293.

Subscripts

D = leading edge diameter in y-z plane, m
L = laminar
T = turbulent
TH = threshold
TR = transition location
x = evaluated at distance x from stagnation point
∞ = freestream conditions, upstream of payload bow shock

I. Introduction

The Hypersonic International Flight Research Experimentation (HIFiRE) program is a hypersonic flight test program executed by the Air Force Research Laboratory (AFRL) and the Australian Defence Science and Technology Organization (DSTO).[1,2] Its purpose is to develop and validate technologies critical to next generation hypersonic aerospace systems. Candidate technology areas include, but are not limited to, propulsion, propulsion-airframe integration, aerodynamics and aerothermodynamics, high temperature materials and structures, thermal management strategies, guidance, navigation, and control, sensors, and weapon system components such as munitions, submunitions, avionics, and weapon system separation. The HIFiRE program consists of extensive ground tests and computation focused on specific hypersonic flight technologies. Each technology program culminates in a flight test. HIFiRE-5 was the second of two flights in the HIFiRE manifest focused on boundary layer transition. The HIFiRE-1 program created an extensive knowledge base regarding transition on axisymmetric bodies that has been summarized in numerous prior publications.[3,4,5,6,7,8,9,10,11,12,13,14] The HIFiRE-5 flight was devoted to measuring transition on a three-dimensional (3D) body.

Extended hypersonic flight with lifting configurations requires improved understanding and prediction of 3D transition. Transition on 3D configurations embodies several phenomena not encountered on axisymmetric configurations like HIFiRE-1, including leading-edge or attachment-line transition and crossflow instabilities (including crossflow interactions with other instability mechanisms shared with axisymmetric flow configurations such as first and second mode instabilities). Very limited hypersonic flight data exist for either phenomena.[15] The need for a better understanding of 3D transition motivated the HIFiRE-5 experiment. This paper describes the HIFIRE-5 mission, launched 23 April 2012 from Andoya, Norway. HIFiRE-5 was a two-stage vehicle. The second stage failed to ignite, preventing the payload from attaining hypersonic speeds. Despite this, surface temperature and pressure data were obtained at subsonic and supersonic Mach numbers, and flight systems including the DMARS IMU, GPS and new data acquisition systems were validated. This paper presents a preliminary overview of the HIFiRE-5 system performance and heat transfer results.

II. Vehicle

The HIFiRE-5 configuration is described in a prior paper.[16] The configuration consisted of a payload mounted atop an S-30 first stage[17] and Improved Orion[18] second stage motor, shown in Figure 1. The term "payload" refers to all test equipment mounted to the second stage booster, including the instrumented test article and additional control and support sections situated between the test article and the second stage motor. The test article consisted of a blunt-nosed elliptic cone of 2:1 aspect ratio, 0.86 meters in length. The vehicle was spin-stabilized. Cant-angle on the first and second-stage fins caused the vehicle to spin passively. Because of this, the payload was rolling throughout the entire trajectory.

The elliptic cone configuration was chosen as the test-article geometry based on extensive previous testing and analysis on elliptic cones.[19,20,21,22,23,24,25,26] This prior work[19,20,21] demonstrated that the 2:1 elliptic cone would generate significant crossflow instability at hypersonic flight conditions and potentially exhibit leading-edge transition. Figure 2 illustrates the elliptic cone geometry and coordinate system.

Figure 3 presents a dimensioned drawing of the payload, including nosetip detail. The half-angle of the elliptic cone test article in the minor axis (x-y) plane was seven degrees, and 13.797 degrees in the major axis. The nose tip cross-section in the minor axis was a 2.5 mm radius circular arc, tangent to the cone ray describing the minor axis, and retained a 2:1 elliptical cross-section to the stagnation point. The elliptic cone major axis diameter was 431.8 mm at the base, and the cone overhung the 355.6 mm diameter second-stage booster in the yaw (x-z) plane. A section with minimal instrumentation blended the elliptical cone cross-section into the circular booster cross section. Small canards for material tests were incorporated on the transition section.[27] A cylindrical can containing GPS, antennas and other equipment resided between the transition section and the Orion booster.

The HIFiRE-5 nosetip construction was similar to that of HIFiRE-1.[30] The nosetip consisted of an iridium-coated TZM tip, followed by a carbon-steel isolator, a stainless steel joiner, and an aluminum frustum. Figure 4 illustrates the nosetip construction. Small backward facing steps were intentionally placed at the nosetip material interfaces to accommodate differential thermal expansion, with the intent that during descent these steps would have closed to present a smooth external surface. These steps were measured using a Mitutoyo Surftest SJ-301 profilometer after the vehicle was assembled at the range. The measured step heights are presented in Figure 5. With the exception of the isolator-joiner joint, all steps were 200 microns or less. Generally, the minor axis presented lower step heights than the major axis.

The 20 mm thick aluminum frustum that served as the primary instrumented surface was constructed from two clamshell-like panels and two leading edges, described in a prior reference.[28] One side of the payload, the 0-90 and 270-360 deg quadrants, was reserved for transition measurement and was devoid of fasteners. The other side of the payload contained countersunk bolts that fastened the closeout panel to the leading edges. This side also contained a small closeout in the nosetip assembly that permitted final assembly of the nosetip (Figure 4). All countersinks were filled flush to the vehicle outer surface with Permatex© Ultra-Copper© RTV gasket compound prior to flight. Figure 6, which shows the payload mounted in a handling fixture, illustrates the row of bolt holes on the closeout side. Prior tests in the NASA Langley 20-inch Mach 6 wind tunnel demonstrated that roughness-induced transition from these fasteners would not propagate to the instrumented side of the payload.[29]

The primary aerothermal instrumentation for HIFiRE-5 consisted of Medtherm Corporation coaxial thermocouples. Type T (copper-constantan) thermocouples were installed in aluminum portions of the aeroshell and Type E (chromel-constantan) were installed in the steel portions. The Medtherm coaxial thermocouples were finished flush with the vehicle surface. These thermocouples were dual-junction thermocouples with one junction at the cone external surface, and the other on the backface. Kulite® pressure transducers measured local static pressures. Several pressure transducers were operated in differential mode to measure differential pressures 180-deg apart on the vehicle to aid in attitude determination. Other Kulite® transducers were sampled at up to 60 kHz to measure high-frequency pressure fluctuations. Several Medtherm 20850-07 Schmidt-Boelter gauges provided direct heat transfer measurements.

The 0-90 degree quadrant of the test article was the primary instrumented surface. It contained thermocouple rays at ϕ=0, 45 and 90-degrees. In addition, three x-stations in this quadrant, x=400, 600 and 800 mm, were instrumented with thermocouples at closely spaced angular locations. The other quadrant on the smooth side of the test article, 270-360 degrees, served as a secondary instrumented surface. It contained the Kulite pressure transducers and a limited amount of thermocouples to provide a symmetry check of the primary instrumentation quadrant.

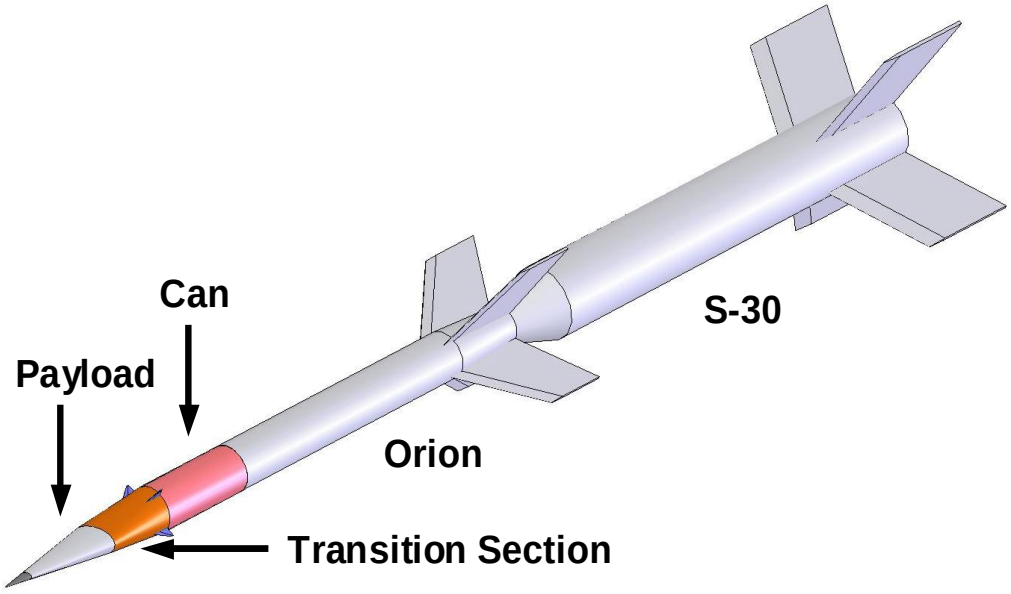

Figure 1 HIFiRE-5 stack.

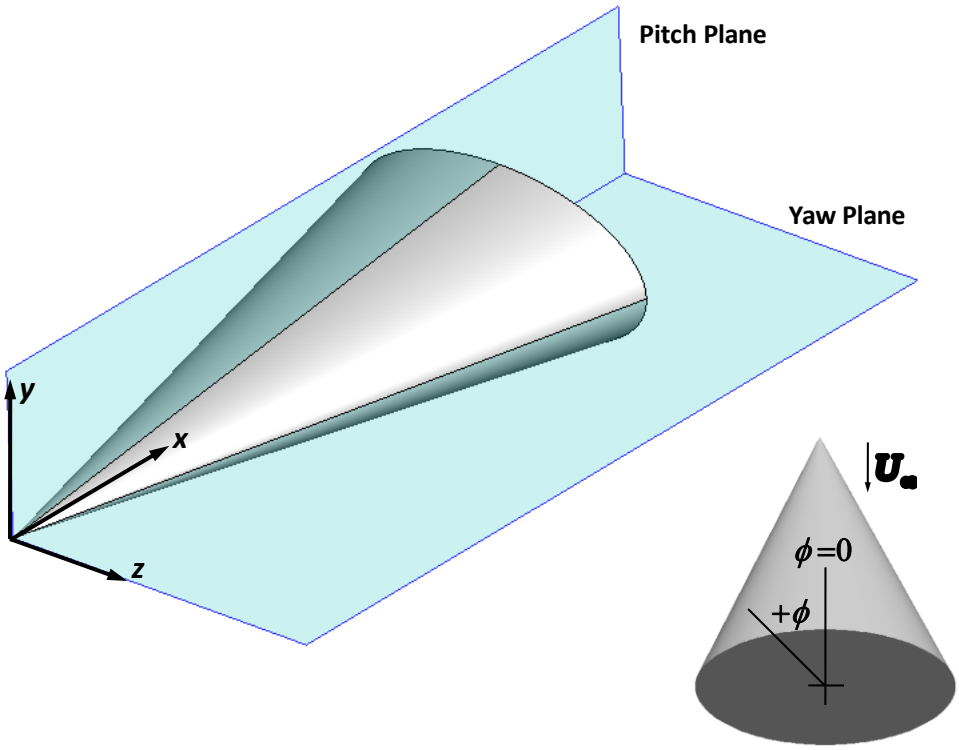

Figure 2 Elliptic cone geometry and coordinate system.

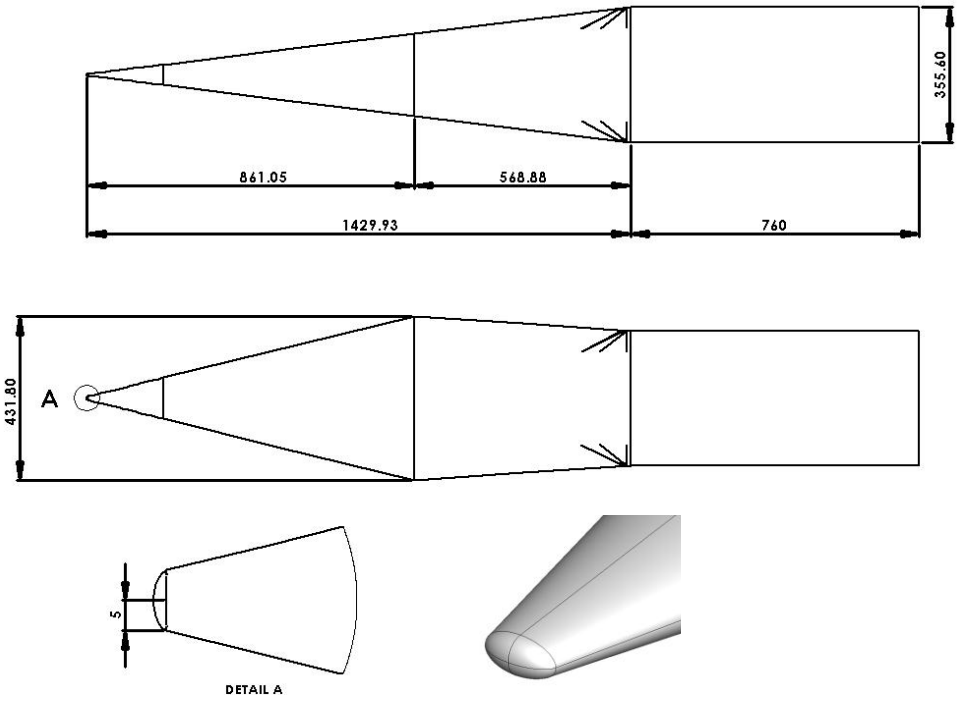

Figure 3 HIFiRE-5 payload, including nosetip detail (dimensions in mm).

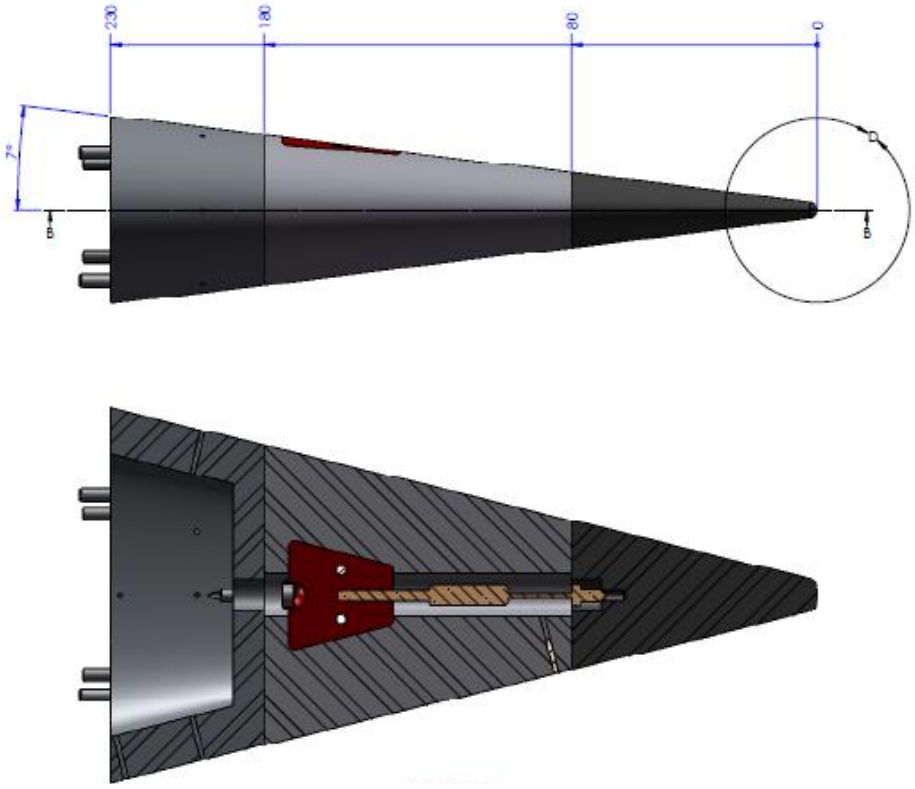

Figure 4 HIFiRE-5 nosetip detail. Dimensions in mm.

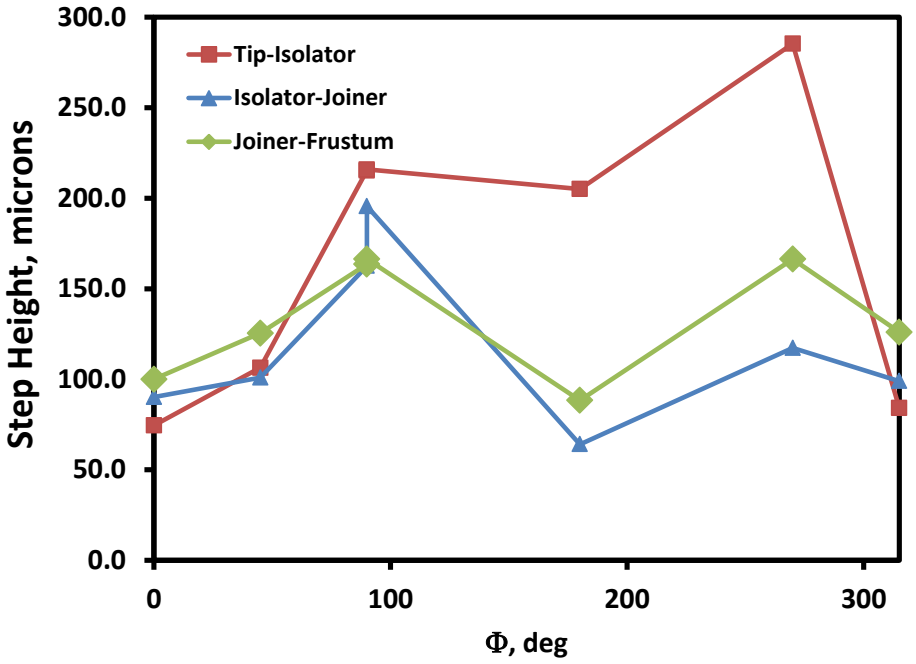

Figure 5 Nosetip assembly cold step heights

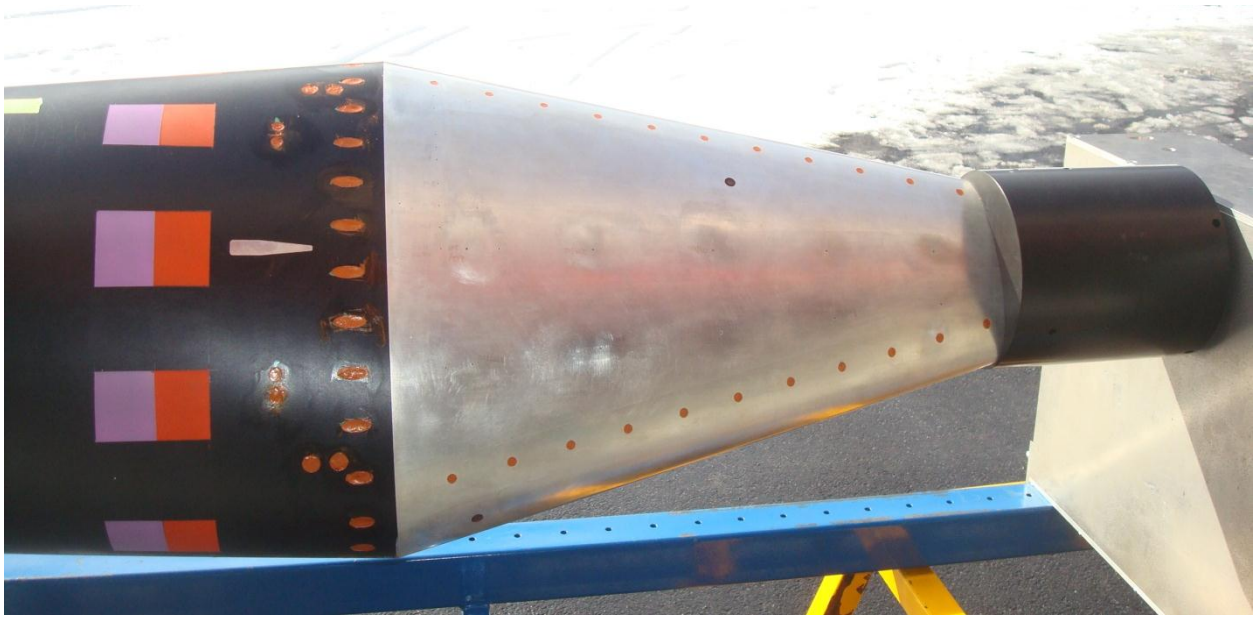

Figure 6 Closeout side of payload showing fasteners (red circles)

III. Trajectory and Vehicle Attitude

HIFiRE-5 was the first HIFiRE flight to use both the Inertial Sciences Digital Miniature Attitude Reference System (DMARS-R) IMU and Ashtech DG14 Global Positioning System receiver. This permitted a cross-check of measured flight parameters between both instruments. In addition, with the flight path angle and azimuth known from either instrument, the IMU could provide vehicle angle of attack and yaw. Figure 7 illustrates the vehicle altitude and velocity as measured by the on-board DMARS inertial measurement unit and GPS. Both instruments showed good agreement. A short drop-out in the GPS signal occurred immediately after launch. Since the second stage failed to light, the maximum altitude achieved was only about 50 km, compared to a planned 300 km apogee. A peak velocity of just over 900 m/s was attained during ascent. Telemetry was received during descent down to 150 meters altitude.

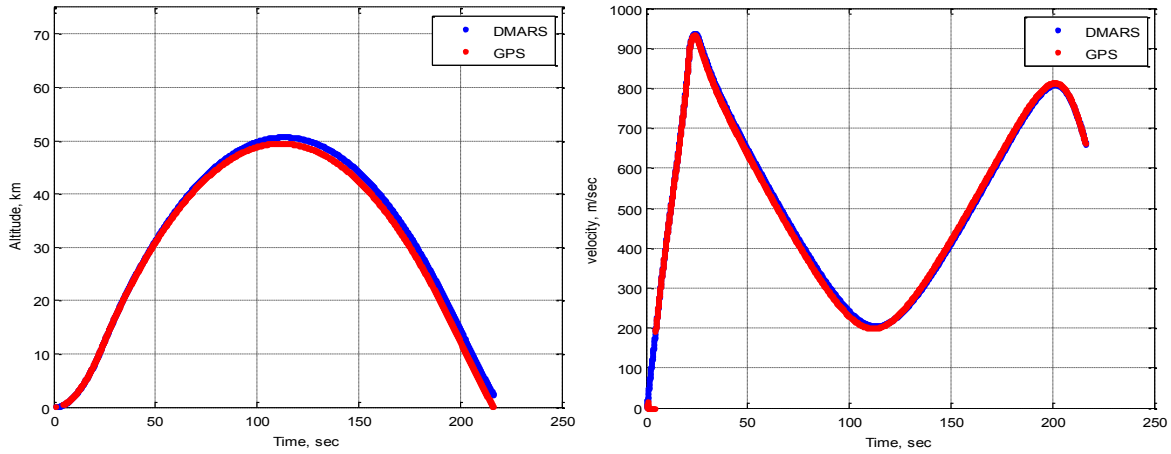

Figure 7 Vehicle altitude (left) and velocity (right)

Figure 5 illustrates the vehicle pitch and azimuth during flight. The red and green points indicate the vehicle flight path angles relative to earth, as derived from the DMARS IMU and the GPS. The blue lines represent the instantaneous vehicle pitch (θ) and azimuth (ψ) orientation as derived from the DMARS IMU. These angles were measured in vertical and horizontal planes, respectively, relative to the local horizontal and north. Both instruments

were in good agreement. Some oscillations in both pitch and azimuth occurred as the vehicle exited the atmosphere (50-100) seconds, and during the vehicle descent (125-175 seconds).

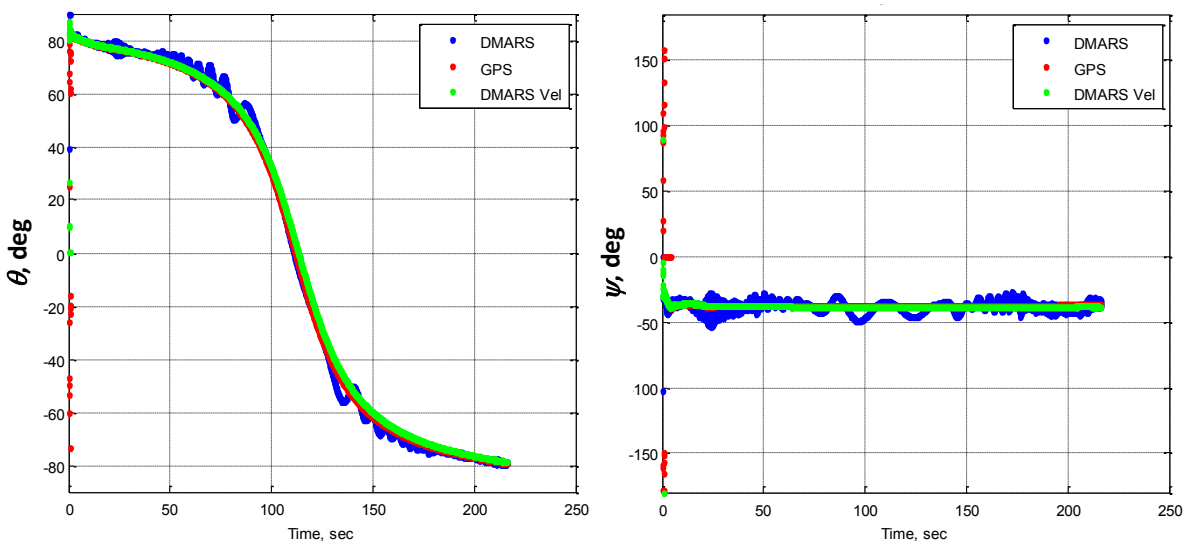

Figure 8 Vehicle pitch angle (left) and azimuth (right)

The vehicle angle of attack and yaw, relative to wind, may be obtained by differencing the vehicle's measured instantaneous pitch or azimuth orientation relative to Earth (derived by integrating angular body rates from the IMU), and the flight path pitch and azimuth relative to earth (derived from the vehicle velocity vector obtained from either the IMU or GPS). This difference produces angle of attack and yaw relative to the flight path. Naming and sign conventions for AoA and yaw are indicated in Figure 9. The vehicle angle of attack and yaw are shown in Figure 10. The vehicle experienced angles of attack approaching four degrees during first-stage burnout and separation. Pitch oscillations continued for a period of time after this. During descent, pitch oscillations damped with time as the vehicle descended. By the time boundary layer transition began to occur during descent, AoA was less than two degrees.

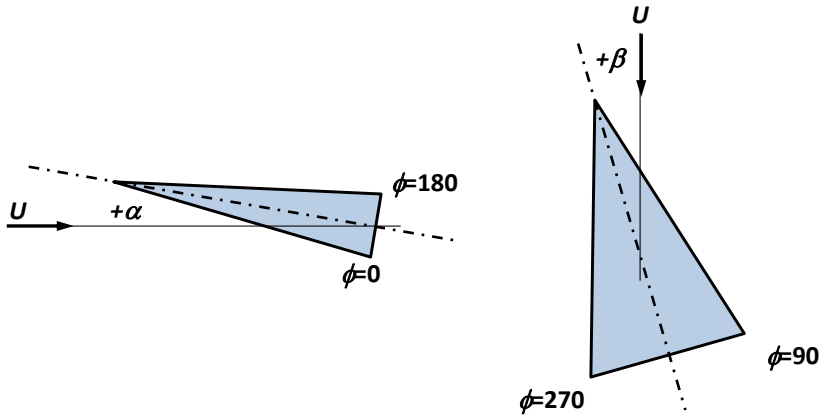

Figure 9 Vehicle attitude angles and conventions

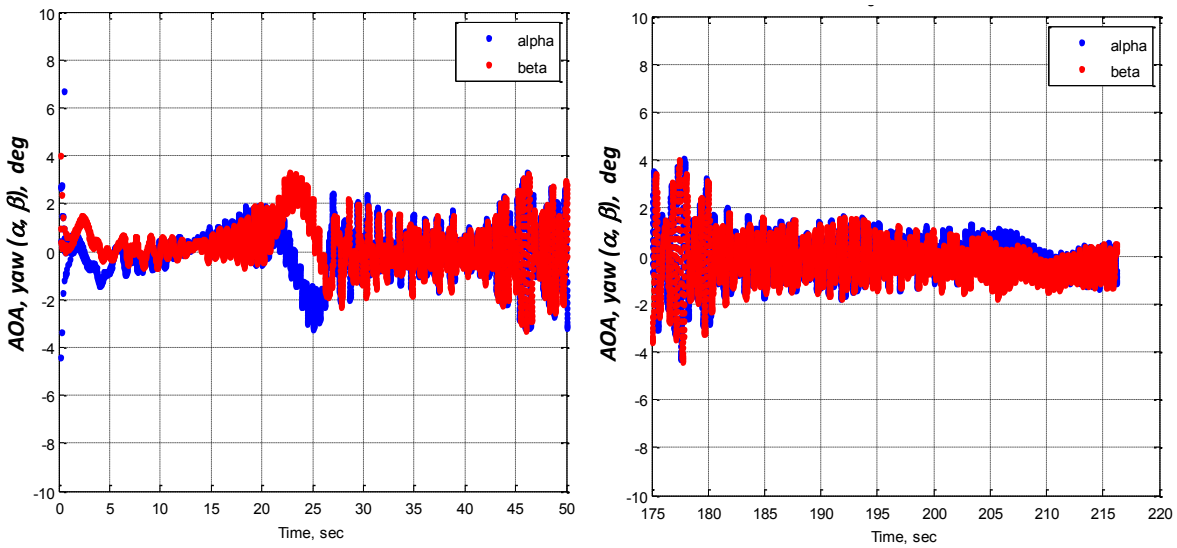

Figure 10 Vehicle angle of attack and yaw during ascent (left) and descent (right)

A combination of balloon and satellite data were used to create a best-estimated-atmosphere (BEA). High-altitude weather balloons were released before and after launch from three stations to provide meteorological data. Balloons were released simultaneously from the range head at Andøya, and from down-range stations at Bjørnaya and Jan Mayen islands. Balloon data were combined with GEOS-5 satellite data to provide conditions during flight at times and locations derived from the GPS. Freestream unit Reynolds number, per meter, is expressed Figure 11 as a function of Mach number during the flight. The peak Mach number of just over three occurred during ascent near first stage burnout. The maximum unit Reynolds number of $3x10^7$ m^{-1} occurred during first stage burn. Mach number during descent was between two and three. Transition occurred during descent at Mach numbers between 2.4 and 2.7.

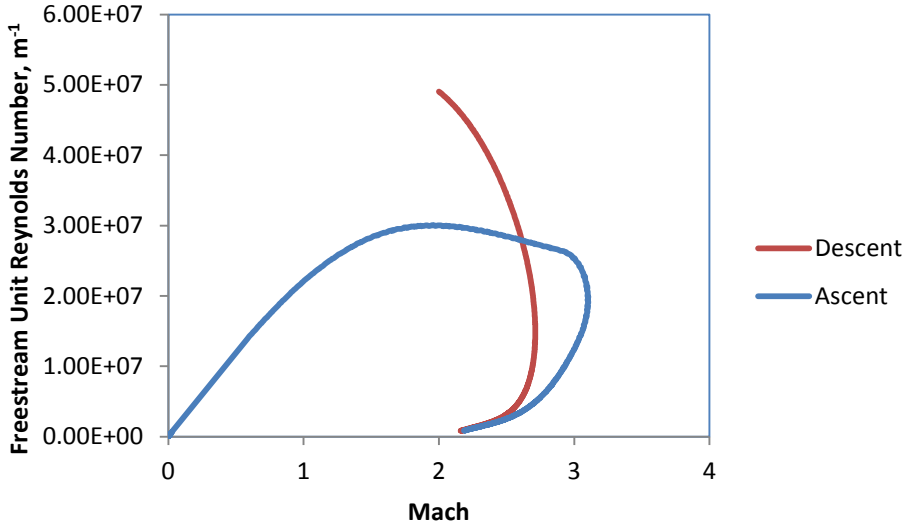

Figure 11 Reynolds number per meter and Mach number during flight

Sample low-bandwidth absolute surface pressure measurements for transducers PLBW30 and PLBW32 are illustrated in Figure 12 and compared to angle of attack to assess the consistency between the two measurements. Both transducers were located on the minor axis at x=0.82 m. PLBW30 was at an angular location of 0-degrees, and PLBW32 was located at 180 deg. With the exception of some oscillations due to vehicle motion and a pressure jump during transonic flight at approximately eight seconds after liftoff, pressure dropped monotonically during ascent. Pressure gradually increased during descent. The mean pressures on opposite sides of the vehicle showed

periods of divergence from each other, for example between about 12 and 23 seconds. This indicates that even though the vehicle was spinning, one side was preferentially offered to windward or leeward, indicative of a phase-locking between the spin and its precession, or a "lunar" motion. This is supported by the angle-of-attack data. AoA during ascent showed periodic fluctuations due to the spin of the vehicle, but these were periodically biased to positive or negative. During descent, AoA fluctuations tended to oscillate about zero.

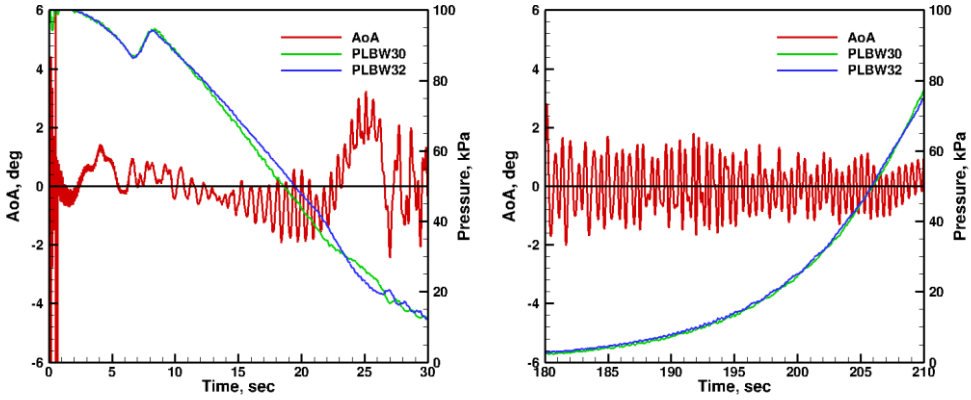

Figure 12 Sample surface pressure measurements during ascent (left) and descent (right)

The AoA and yaw derived from the DMARS IMU may be further confirmed by comparing them to differential pressures. Differential pressures were measured during flight by differential pressure transducers connected to two ports located 180-deg opposite each other on the vehicle. The differential transducer PLBW21d was located on the minor axis and primarily sensitive to AoA, and PLBW25D was located on the major axis and primarily sensitive to yaw. Both were located at x=0.775 m. Figure 13 compares pressures measured with these transducers to AoA and yaw. Differential pressures were normalized by freestream static pressure. The ascent AoA and yaw qualitatively resembled the respective differential pressures. This was also true during descent, although the correlation between vehicle attitude and differential pressure was less pronounced. There was generally good qualitative agreement to about 195 seconds. After this time, additional fluctuations appeared in the pressure signal, although the overall envelope of the differential pressures was similar to that of the body angles.

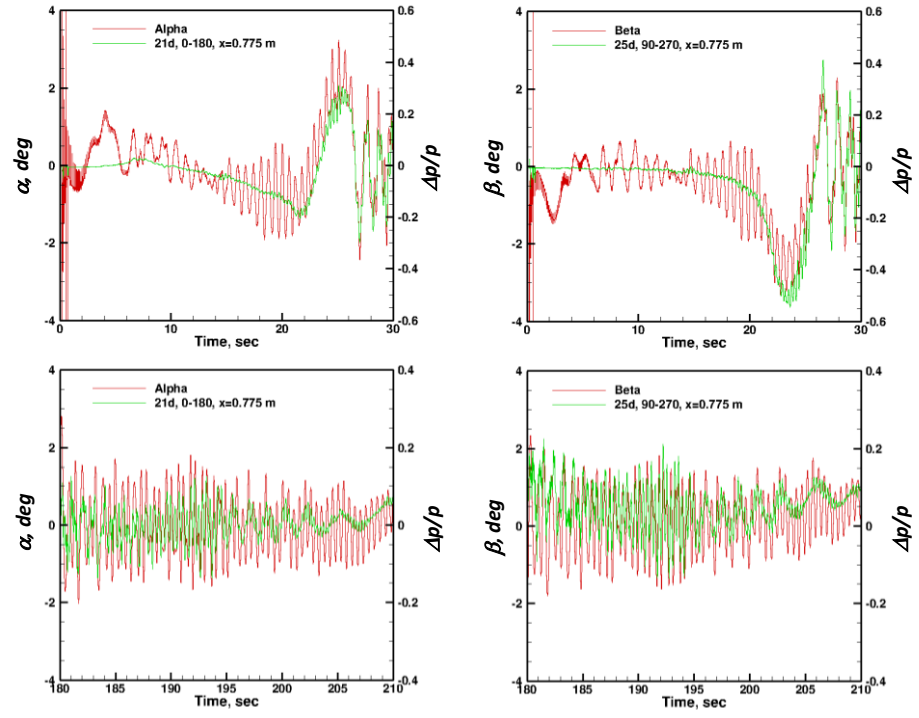

Figure 13 Ascent (top) and descent (bottom) AoA (left) and yaw (right), compared to differential pressures.

IV. Transition Results

Sample heat transfer measurements at upstream and downstream locations on the major and minor axes illustrate major features of the transition behavior. Heat transfer results were obtained by applying an inverse heat transfer solution to thermocouple temperature measurements from the front face (wetted surface) and back face (interior surface) of the aeroshell.[30] The analysis presented in this paper is a 1D inverse heat transfer solution, including curvature terms.[30] Based on HIFiRE-1 results, axial and lateral conduction effects were expected to be minimal, and this will be assessed quantitatively at a later date. Measured front-face and back-face temperatures were used as boundary conditions for the inverse analysis. The resulting heat transfer rates were smoothed using a 200 point (0.25 sec) moving average. Front and back-face thermocouples were zero-shifted to the same temperature prior to launch to create a zero heat-flux starting condition. Ambient temperature at launch was approximately 280 K. Heat generation within the payload was neglected in the thermal analysis. Total payload electrical power consumption was approximately 240W, but most of that was confined to the payload support module, or "can" aft of the payload, and some of this power was radiated through telemetry antennas. The primary source of power dissipation in the elliptic cone test article itself was the sensor collection boards. This power generation was estimated to be less than 10W.

Measured heat transfer was compared to predicted fully laminar and fully turbulent heat transfer rates to graphically indicate when transition occurs. Laminar and turbulent heating rates were computed using a correlation developed from sharp elliptic cone wind tunnel data.[19] These predicted levels are approximate and only intended to illustrate trends.

Figure 14 (left) presents heat transfer on the major axis during ascent and descent. Predicted turbulent heating levels were well above measured heating rates, but this quantitative disagreement was not unexpected given the approximate nature of the prediction. Both transducers were located on the vehicle leading edge (major axis) at ϕ=90 deg. Sensor 051 is located at x=0.35 m, and sensor 281 is located at x=0.85 m. Heat transfer peaked at about t=21 seconds and then decreased as first-stage thrust tailed off. The heat transfer began to drop from turbulent to laminar trends at t=25-26 seconds. Shortly after this, at about t=27.2 seconds, heating returned briefly to turbulent trends, then resumed its progression to laminar levels. This unsteady transition progress was coincident with AoA and yaw excursions caused by first-stage separation.

It is noteworthy that the transition events on the two transducers occurred almost simultaneously. The initial departure from turbulent heating levels occurred first on the upstream transducer, at t=24.8 seconds and a length Reynolds number of 3.4×10^6. The downstream transducer registered a similar departure at t=25.9 seconds and a Reynolds number of 12.1×10^6. This rapid movement of the transition front is typical of a tripped transition, and is similar to behavior observed on HIFiRE-1 during ascent.[30] The most likely source of the trip was the nosetip steps described above.

On at least one sensor, 281 (x=0.85 m), the heating level after ascent did not drop to fully laminar levels, but remained at an elevated level. The most likely cause for this bias was a shift in one of the thermocouples. At t=150 seconds, which is near the minimum temperature condition between ascent and descent, the measured front-face / back-face temperature differential at this location was 2.2 deg C. All descent heat transfer results presented below were zero-shifted to zero heat transfer at t=150 seconds.

During descent, both leading-edge transducers showed a steady increase in heat transfer beginning near t=170 seconds consistent with expected laminar heating trends. A sharp increase in heating rates occurred near t=198 seconds. This rapid increase in heating rate occurred on the downstream transducer slightly before it occurred on the upstream transducer. This event is consistent with a transition from laminar to turbulent flow, proceeding from the aft region of the elliptic cone toward the front. The entire leading edge transitioned rapidly, as it did during ascent. The aft-most thermocouple registered transition at t=197.62 seconds (Re_x=10.6×10^6), and the forward thermocouple transitioned at 198.54 seconds (Re_x=4×10^6). This rapid transition movement again indicates a tripping event.

Previous work suggested that leading edge roughness effects might be correlated with local diameter-based Reynolds number.[28] During ascent, earliest (highest Reynolds number) leading edge transition occurred when Re_D reached 2.1×10^5 at the most upstream (nosetip / isolator) joint. During descent, latest (highest Reynolds number) leading edge transition occurred when the diameter Reynolds number at the most upstream joint was 1.8×10^5. Although not conclusive, these numbers are consistent with maximum values of Re_D at which laminar flow can still be maintained in the presence of large roughness. Typical values derived hypersonic wind tunnel experiments are from Bushnell and Huffman[31] (Re_D =2×10^5) and Murakami et al.[32] ($1.5 \times 10^5 < Re_D < 3.3 \times 10^5$).

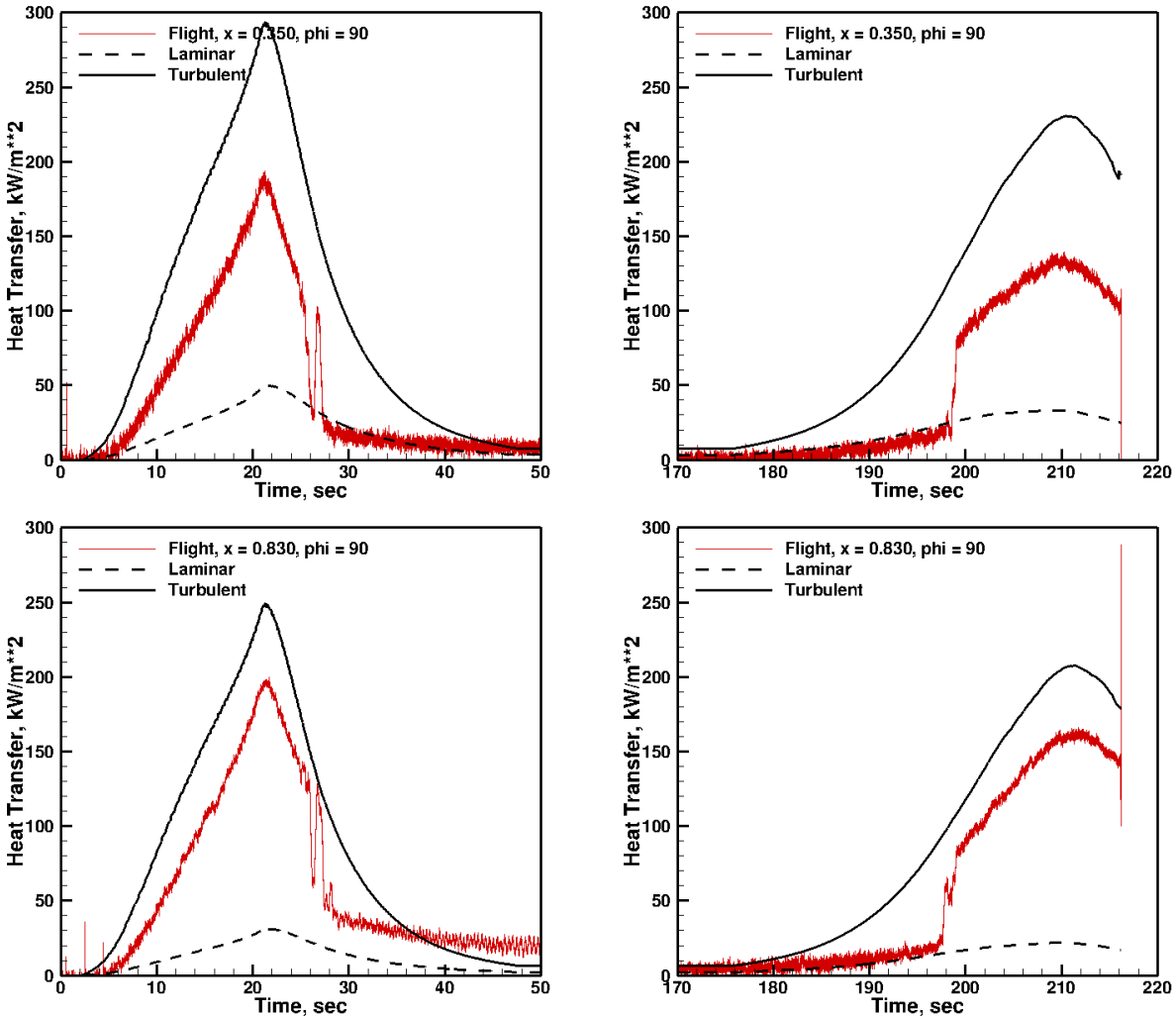

Figure 14 Heat transfer at upstream (top) and downstream (bottom) locations on the leading edge (major axis) during ascent (left) and descent (right)

The minor axis (centerline) transitioned at a lower Reynolds number than the leading edge, which is consistent with prior CFD[33,34] and wind tunnel measurements[28,29] at hypersonic conditions that indicated that the centerline is more unstable and prone to lower Reynolds number transition. Centerline transition also showed a more gradual progression over time than the leading edge transition. Heat transfer as a function of time at upstream and downstream locations on the minor axis is illustrated in Figure 15. These transducers were located at similar *x*-locations as the leading edge transducers, whose results are illustrated in Figure 14. Upstream transducer 047 was located at x=0.35 and downstream transducer 277 was located at x=0.83. Overall heat transfer levels for the Figure 15 transducers were lower than those shown in Figure 14, consistent with the greater radius of curvature and smaller cone angle on the minor axis. Heating rates remained at turbulent levels well through ascent. It appears that the upstream thermocouple (047, x=0.35) may have begun to register laminar levels shortly after t=30 seconds, but heating rates at this time were low, and signal-to-noise ratio is poor. During descent, heat transfer on the downstream thermocouple (277, x=0.83) tracked turbulent trends as early as t=182 seconds. Again, since heating rates at this condition were low, and there was little difference between laminar and turbulent levels, the precise transition time is difficult to discern. Heat transfer on the upstream thermocouple during descent however, did not show a marked departure from laminar levels until approximately t=191 seconds. The transition process on the centerline was clearly more gradual than on the leading edge.

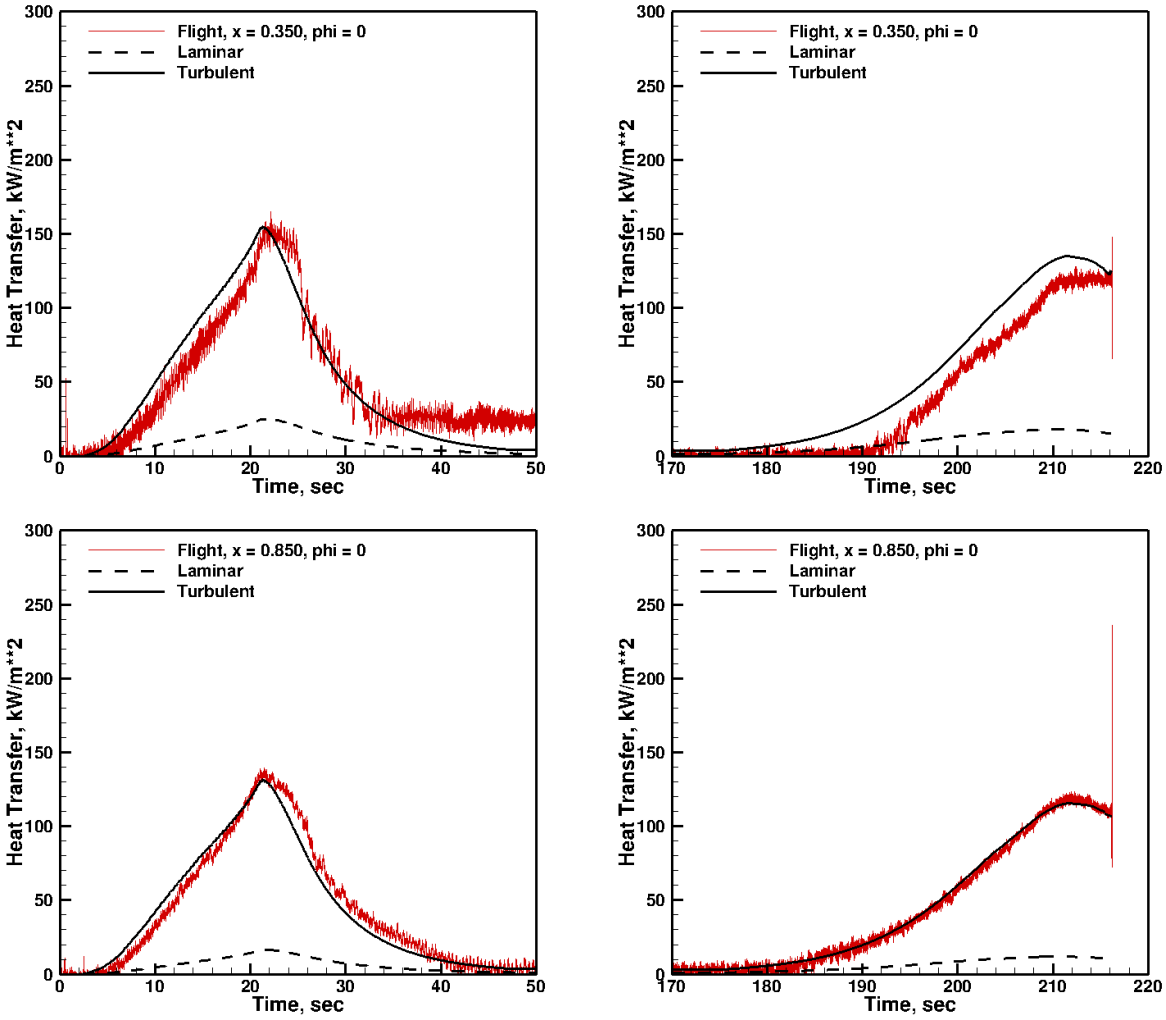

Figure 15 Heat transfer for upstream (top) and downstream (bottom) transducers on the minor axis during ascent (left) and descent (right)

Spanwise cuts of transition Reynolds numbers, obtained as a function of angular location around the test article with *x*-station as a parameter, provide an overall picture of the transition front. Figure 16 shows results for selected transducers at three *x*-locations during descent. The descent portion of the trajectory was chosen for this analysis since the angles of attack were lower, and the data are easier to interpret. The selection of transition times was somewhat subjective for two reasons. First, for early transition times near the centerline (ϕ=0), the difference between laminar and turbulent heating is small and the first departure from laminar heating is somewhat indistinct. Also, as noted above, in some cases the transition process was intermittent, showing one or more departures from and returns to laminar heating rates. For this reason, early and late transition times were determined, and these were used to determine an average transition time. Early transition corresponds to the first discernible departure from laminar heating rates, and late corresponds to the final discernible departure from laminar flow, after which the flow remained turbulent. The early and late bounds are indicated by dashed lines in Figure 16. For clarity, only the bounds on the most downstream station, *x*=800 mm, are indicated. Also, transition results from thermocouples on the secondary instrumentation quadrant are shown as open symbols in Figure 16 to demonstrate lateral transition symmetry. The angular location of instrumentation on the secondary quadrant has been shifted by 360 degrees in Figure 16, so that the instrument locations coincide with their mirror image location on the primary quadrant.

Given the conical shape of the test article and minor variations in Mach number during descent, smooth-body transition Reynolds number should be approximately equal at any angular location, barring nose bluntness effects or

variations in the vehicle orientation. This was true for locations away from the leading edge. The variation between early and late transition at x=800 mm varies by about +/-15%, and the average transition location at the other x-stations generally fell within these bounds. This behavior indicates that the acreage transition appears to have been uninfluenced by tripped transition at the leading edge. The transition pattern agrees qualitatively with patterns observed in hypersonic wind tunnel experiments and computations[33,34] for hypersonic flight Mach numbers, with centerline transition occurring earlier than leading edge transition, due to the more unstable centerline boundary layer.

The region near the leading edge of the test article showed a non-similar transition behavior, as expected based upon inspection of individual transducer results described above. At x=600 mm, transition at angular locations greater than ϕ=70-deg. appear compromised. At x=400 mm, locations for ϕ>60 deg. are non-similar. This transition pattern suggests a tripped transition near the leading edge that spilled inboard and contaminated an increasing portion of the acreage as time progressed.

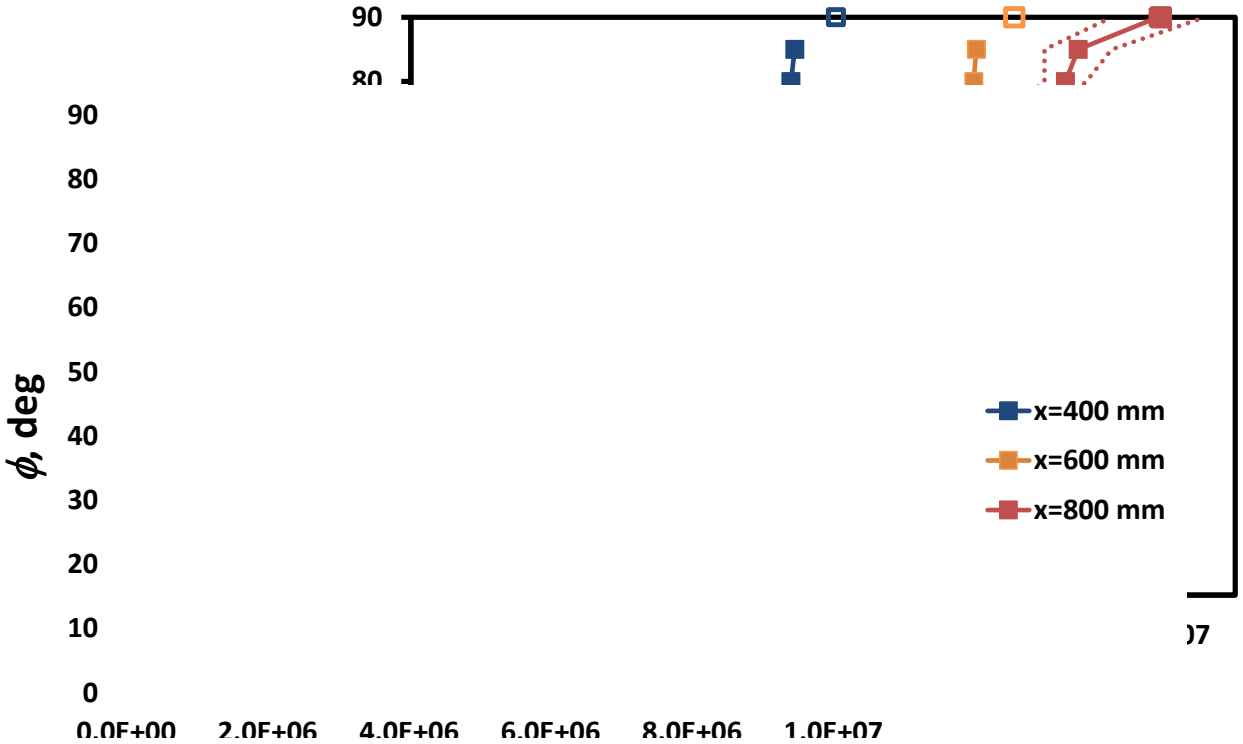

Figure 16 Transition Reynolds numbers during descent. Open symbols: secondary instrumentation quadrant (360<ϕ<270), reflected in ϕ. Dashed lines – early and late transition limits at x=800 mm.

Transition data obtained at varying x-locations with angular location as a parameter were used to derive transition Reynolds number in a more systematic fashion. Figure 17 shows the transition location as a function of freestream Reynolds number for several angular locations. Transition was defined in this case as the thermocouple location where the heating rate exceeded a given threshold. The threshold was selected as the local predicted laminar heating rate plus 30% of the difference between predicted laminar and turbulent rates, i.e., $\dot{q}_{TH} = 0.3(\dot{q}_T - \dot{q}_L) + \dot{q}_L$. Along these four densely instrumented rays, the thermocouples were installed in 50-mm increments from x = 200 to 900 mm, hence the granularity and limits of the indicated transition locations. For the ϕ=0 and 45-deg locations, a line of constant Re_{TR} was fit to the data using the Matlab® function "fit" from the Curve Fitting Toolbox. The ϕ=90 and 270-deg leading-edge rays were not curve fit, since as noted above, transition on these rays did not appear to be correlated by a constant transition Reynolds number. These curve fits indicate a transition Reynolds number of 2.2x10^6 on the ϕ=0 deg. ray and 3.1 x10^6 on the ϕ=45 deg. ray. The results in Figure 17 at x=400, 600 and 800 mm are similar to the transition Reynolds numbers for ϕ=0, 45 and 90 degrees plotted in Figure 16.

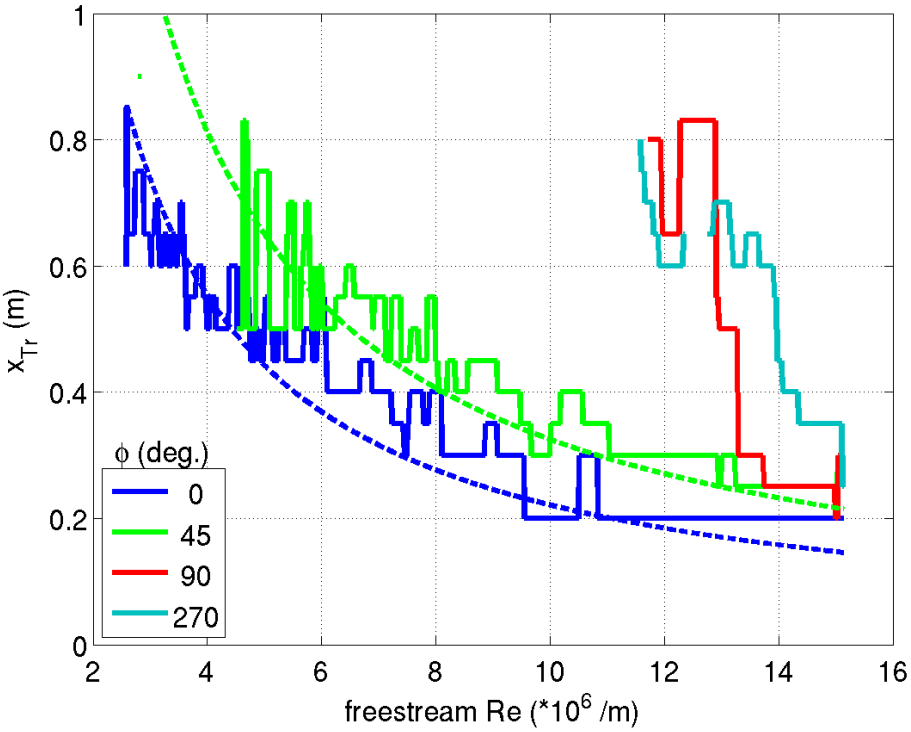

Figure 17 Transition location as a function of freestream Reynolds number at various angular locations.

V. Conclusions and Future Work

Although HIFiRE-5 failed to reach its desired hypersonic flight conditions, the experiment acquired useful supersonic transition data. The experiment demonstrated that meaningful supersonic transition data may be obtained by using surface-mounted instrumentation on a spin-stabilized sounding rocket, even on a three-dimensional body undergoing some attitude excursions. In addition, the flight demonstrated GPS and IMU hardware new to the HIFiRE program. Although transition near the leading-edge appeared to have been affected by backward facing steps on the nosetip, the rest of the payload did not appear to demonstrate any gross effects of tripping. Since the nosetip steps were measured prior to flight, it is hoped that the leading edge data may be used to determine leading edge trip correlations for supersonic flight.

Generally, the descent portion of the trajectory provided lower angles of attack and cleaner transition behavior than did ascent. The overall transition front on the vehicle, with the exception of leading edge transition, showed a pattern similar to wind tunnel experiments and CFD, with a low-Reynolds number transition on the centerline, and higher Reynolds number transition on the leading edge. The leading edge diameter Reynolds numbers corresponding to leading edge transition were consistent with similar values measured in wind tunnel tests.

Further analysis of all the HIFiRE-5 sensors will provide a fuller picture of the test article transition behavior. Conduction analysis of the leading edge will quantify the effects of lateral conduction on heat transfer. Navier-Stokes analysis of selected trajectory points will aid in determining leading edge trip correlations and will help to validate vehicle attitude measurements by comparing measured and computed surface pressures. These computations will include cases with non-zero yaw and angle of attack. Analysis of additional thermocouples and direct-read heat transfer gauges will provide more detailed maps of the transition front. These data will be combined with instantaneous attitude data to examine the effect of body attitude on transition, including the ascent phase. High bandwidth pressure data will be analyzed for spectral content and broad-band RMS.

Acknowledgments

This work was supported by the United States Air Force Research Laboratory and the Australian Defence Science and Technology Organisation and was carried out under Project Agreement AF-06-0046. Many thanks are extended to the Andoya Rocket Range of Norway and DLR/Moraba, and all members of the DSTO AVD Team Brisbane. The authors gratefully acknowledge the efforts and support of Douglas Dolvin, AFRL/RQH and John Schmisseur of

the Air Force Office of Scientific Research, AFOSR/RSA. Mary Bedrick of Detachment 3 Air Force Weather Agency generated the best-estimated atmosphere. The 1st stage rocket motor was procured from CTA Instituto de Aeronáutica e Espaço (IAE, Brazil) by the DLR.

References

[1] Dolvin, D. "Hypersonic International Flight Research and Experimentation (HIFiRE) Fundamental Science and Technology Development Strategy," AIAA Paper 2008-2581, April 2008.

[2] Dolvin, D. J., "Hypersonic International Flight Research and Experimentation Technology Development and Flight Certification Strategy," AIAA paper 2009-7228, October 2009.

[3] Kimmel, R. L., Adamczak, D., Gaitonde, D., Rougeux, A., Hayes, J. R., "HIFiRE-1 Boundary Layer Transition Experiment Design," AIAA paper 2007-0534, January 2007.

[4] Wadhams, T. P., MacLean, M. G., Holden, M.S., and Mundy, E., "Pre-Flight Ground Testing of the Full-Scale FRESH FX-1 at Fully Duplicated Flight Conditions," AIAA paper 2007-4488, June 2007.

[5] Johnson, H. B., Alba, C. R., Candler, G. V., MacLean, M., Wadhams, T, and Holden, M. "Boundary Layer Stability Analysis of the Hypersonic International Flight Research Transition Experiments," AIAA Journal of Spacecraft and Rockets, vol. 45, no. 2, March-April 2008, pp228-236.

[6] Holden, M. S., Wadhams, T. P., MacLean, M., "Experimental Studies in the LENS Supersonic and Hypersonic Tunnels for Hypervelocity Vehicle Performance and Code Validation," AIAA paper 2008-2505, April 2008.

[7] Kimmel, R. L., "Aerothermal Design for the HIFiRE-1 Flight Vehicle," AIAA paper 2008-4034, June 2008.

[8] Casper, K. M., Wheaton, B. M., Johnson, H. B., and Schneider, S. P., "Effect of Freestream Noise on Roughness-Induced Transition at Mach 6," AIAA paper 2008-4291 June 2008.

[9] Kimmel, R. L., "Roughness Considerations for the HIFiRE-1 Vehicle," AIAA Paper 2008-4293, June 2008.

[10] Alba, C. R., Johnson, H. B., Bartkowicz, M. D., Candler, G. V., and Berger, K. T. "Boundary-Layer Stability Calculations for the HIFiRE-1 Transition Experiment," *AIAA Journal of Spacecraft and Rockets*, vol. 45, no. 6, November-December 2008, pp. 1125-1133.

[11] Wadhams, T. P., Mundy, E., MacLean, M. G., and Holden, M. S., "Ground Test Studies of the HIFiRE-1 Transition Experiment Part1: Experimental Results," *AIAA Journal of Spacecraft and Rockets*, vol. 45, no. 6, November-December 2008, pp. 1134-1148.

[12] MacLean, M., Wadhams, T., Holden, M., and Johnson, H., "Ground Test Studies of the HIFiRE-1 Transition Experiment Part 2: Computational Analysis," *AIAA Journal of Spacecraft and Rockets*, vol. 45, no. 6, November-December 2008, pp. 1149-1164.

[13] Berger, K. T., Greene, F. A., Kimmel, R. L., Alba, C., and Johnson, H., "Erratum on Aerothermodynamic Testing and Boundary-Layer Trip Sizing of the HIFiRE Flight 1 Vehicle," AIAA Journal of Spacecraft and Rockets, vol. 46, no., 2, March-April, 2009, pp. 473-480.

[14] Adamczak, D., Alesi, H., Frost, M., "HIFiRE-1: Payload Design, Manufacture, Ground Test, and Lessons Learned," AIAA paper 2009-7294, October 2009.

[15] Malik, M. R., Li, F., Choudhari, M., "Analysis of Crossflow Transition Flight Experiment aboard the Pegasus Launch Vehicle," AIAA paper 2007-4487, June 2007.

[16] Kimmel, R. L, Adamczak, D., Berger, K., and Choudhari, M., "HIFiRE-5 Flight Vehicle Design," AIAA paper 2010-4985, June 2010

[17] Palmerio, A. F.; Peres da Silva, J. P. C.; Turner, P.; Jung, W., "The development of the VSB-30 sounding rocket vehicle," in 16th ESA Symposium on European Rocket and Balloon Programmes and Related Research, 2 - 5 June 2003. Ed.: Barbara Warmbein. ESA SP-530, Noordwijk: ESA Publications Division, 2003, p. 137 – 140.

[18] "NASA Sounding Rocket Program Handbook," 810-HB-SRP, Sounding Rockets Program Office, Suborbital & Special Orbital Projects Directorate, Goddard Space Flight Center, Wallops Island Flight Facility, June 2005.

[19] Kimmel, R. L., and Poggie, J., "Transition on an Elliptic Cone at Mach 8," American Society of Mechanical Engineers ASME FEDSM97-3111, June 1997.

[20] Kimmel, R. L., and Poggie, J., "Three-Dimensional Hypersonic Boundary Layer Stability and Transition," Air Force Research Laboratory Technical Report, WL-TR-97-3111, December 1997, Wright-Patterson Air Force Base, Ohio.

[21] Kimmel, R. L., and Poggie, J., Schwoerke, S. N., "Laminar-Turbulent Transition in a Mach 8 Elliptic Cone Flow," AIAA Journal, vol. 37, no. 9, Sep. 1999, pp. 1080-1087.

[22] Schmisseur, J. D., "Receptivity of the Boundary Layer on a Mach-4 Elliptic Cone to Laser-Generated Localized Freestream Perturbations," Doctoral Dissertation, Purdue University Aerospace Sciences Laboratory, December 1997.

[23] Holden, M., "Experimental Studies of Laminar, Transitional, and Turbulent Hypersonic Flows Over Elliptic Cones at Angle of Attack," Air Force Office of Scientific Research Technical Report AFRL-SR-BL-TR-98-0142, Bolling Air Force Base, DC, 1998.

[24] Schmisseur, J. D., Schneider, S. P., and Collicott, S. H., "Receptivity of the Mach 4 Boundary Layer on an Elliptic Cone to Laser-Generated Localized Freestream Perturbations," AIAA paper 1998-0532, January 1998.

[25] Schmisseur, J. D., Schneider, S. P., and Collicott, S. H., "Response of the Mach 4 boundary layer on an elliptic cone to laser-generated freestream perturbations," AIAA paper 1999-0410, January 1999.

[26] Lyttle, I. J., and Reed, H. L., "Use of Transition Correlations for Three-Dimensional Boundary Layers Within Hypersonic Flows," AIAA-95-2293, June 1995.
[27] Löhle,S., Böhrk, H., Fuchs, U., Kraetzig, B., and Weihs, H., "Three-Dimensional Thermal Analysis of the HIFiRE-5 Ceramic Fin," AIAA paper 2012-5920, September 2012.
[28] Kimmel, R. L, Adamczak, D., Berger, K., and Choudhari, M., "HIFiRE-5 Flight Vehicle Design," AIAA paper 2010-4985, June 2010.
[29] Berger, K. T., Rufer, S. J., Kimmel, R. and Adamczak, D., "Aerothermodynamic Characteristics of Boundary Layer Transition and Trip Effectiveness of the HIFiRE Flight 5 Vehicle," AIAA paper 2009-4055, June 2009.
[30] Kimmel, R. L., Adamczak, D., and Brisbane DSTO-AVD Team, "HIFiRE-1 Preliminary Aerothermodynamic Experiments," AIAA paper 2011-3413, June 2011.
[31] Bushnell, D. M., and Huffman, J. K., "Investigation of Heat Transfer to Leading Edge of a 76° Swept Fin With and Without Chordwise Slots and Correlations of Swept-Leading-Edge Transition Data for Mach 2 to 8," NASA TM X-1475, December 1967.
[32] Murakami, A., Stanewsky, E., and Krogman, P., "Boundary-layer Transition on Swept Cylinders at Hypersonic Speeds," *AIAA Journal*, vol. 34, no. 4, April 1996, pp. 649-654.
[33] Choudhari, M., Chang, C.-L., Jentink, T., Li, F., Berger, K., Candler, G., and Kimmel, R., "Transition Analysis for the HIFiRE-5 Vehicle," AIAA paper 2009-4056, June 2009.
[34] Gosse, R., Kimmel, R. L., and Johnson, H. B., "CFD Study of the HIFiRE-5 Flight Experiment," AIAA paper 2010-4854, June 2010.